CHAPTER 4

Results

4.1 Estimated Shear Wave Velocity

Shear wave velocity (V_S) of D-36 well was predicted using compressional wave velocity (V_P) because the shear sonic log of this well is available at deeper section only (lower FM1 to FM0). The estimation was used empirical relation of V_P and V_S (Greenberg and Castagna, 1992) and was modified to match the existing well log data of this area. In the result, the estimated V_S log of D-36 which is used in this study was combined between the existing data (pink curve) and the estimated data from V_P log (pale green curve). In V_P versus V_S crossplot, the estimated data is represented to linear relationship following the equation of shale and sandstone in Chapter 3.2.2, and the existing data of FM1 and FM0 are represented to the scattering points (Figure 4-1).

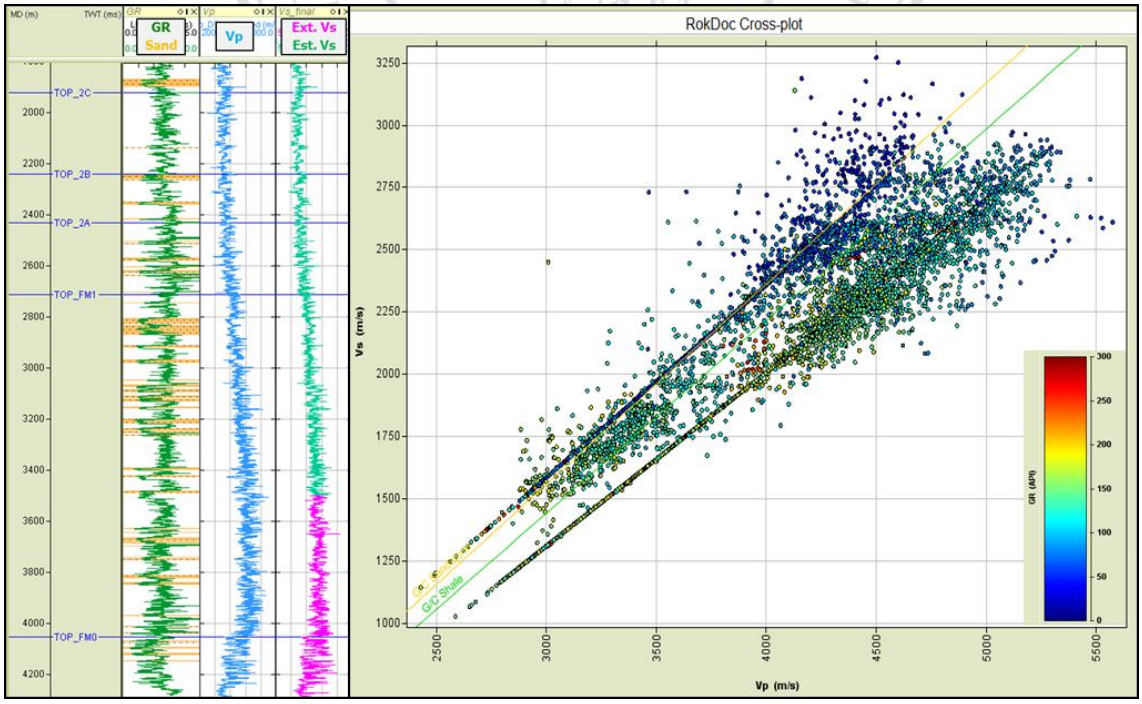

Figure 4-1. Results of the estimated V_S and V_P - V_S crossplot of D-36, V_P log (blue curve), existing V_S log (pink curve), estimated V_S log (pale green curve)

4.2 Sonic Log Calibration and Well Correlation

4.2.1 Sonic Log and Checkshot Calibration

Sonic log calibration which is correlation between checkshot and P-wave sonic log in wells by adjusting time of sonic log to match with smoothed checkshot times is done for four wells in the study area. The results of residual drift and polynomial fit after correlation are represented in Table 4-1. The greatest amount of drift is observed at G-29 well location because checkshot or VSP is not available, so shared checkshot of nearby well is used for calibration. Therefore, the G-29 well would not be used for seismic inversion due to it is located on the unavailable seismic data area.

Table 4-1. Minimum and maximum residual drift after sonic log calibration using polynomial fit to checkshot data

Well	Residual Drift		Polynomial Fit Order
	Minimum	Maximum	
S-2	-2.98	2.39	4
R-2	-5.54	5.99	4
D-36	-8.50	6.19	3
G-29	-14.96	16.55	3

4.2.2 Seismic and Well Correlation

It is crucial to conduct seismic-well tie depth-time conversion and residual static correction. The wavelet that was applied to create synthetic traces for each well is 180° phase rotation of 25 Hz of Ricker wavelet to match seismic polarity of stacking volume. Only bulk shift was applied to each well for matching the depth-to-time data of well logs to the seismic times which is presented in Table 4-2. To create synthetic traces, a wavelet was extracted from seismic data or was deterministically generated, and then gets better matching in seismic-well tie (Figures 4-2 to 4-4). Other wavelets were obtained using wells for generating inversion model and inversion analysis which its phase should be the phase of seismic data at working interval (Figure 4-5).

Table 4-2. Bulk shift and correlation coefficient of each well

Well	Bulk Shift (ms)	Correlation Coefficient	Wavelet	
			Frequency (Hz)	Phase (°)
S-2	17	0.755	25	180
R-2	13	0.534	25	180
D-36	14	0.654	25	180

These wavelets were used for well to seismic correlation. To perform seismic inversion correctly the extracted zero phase (or 180 degrees phase) wavelets will not be used because real seismic data is not the theoretical zero phase. The wavelet for inversion should be rotated the phase to symmetric shape of cross-correlation. Moreover, to do the pre-stack inversion, it is crucial to extract a few numbers of wavelets based on the number of angle gathers.

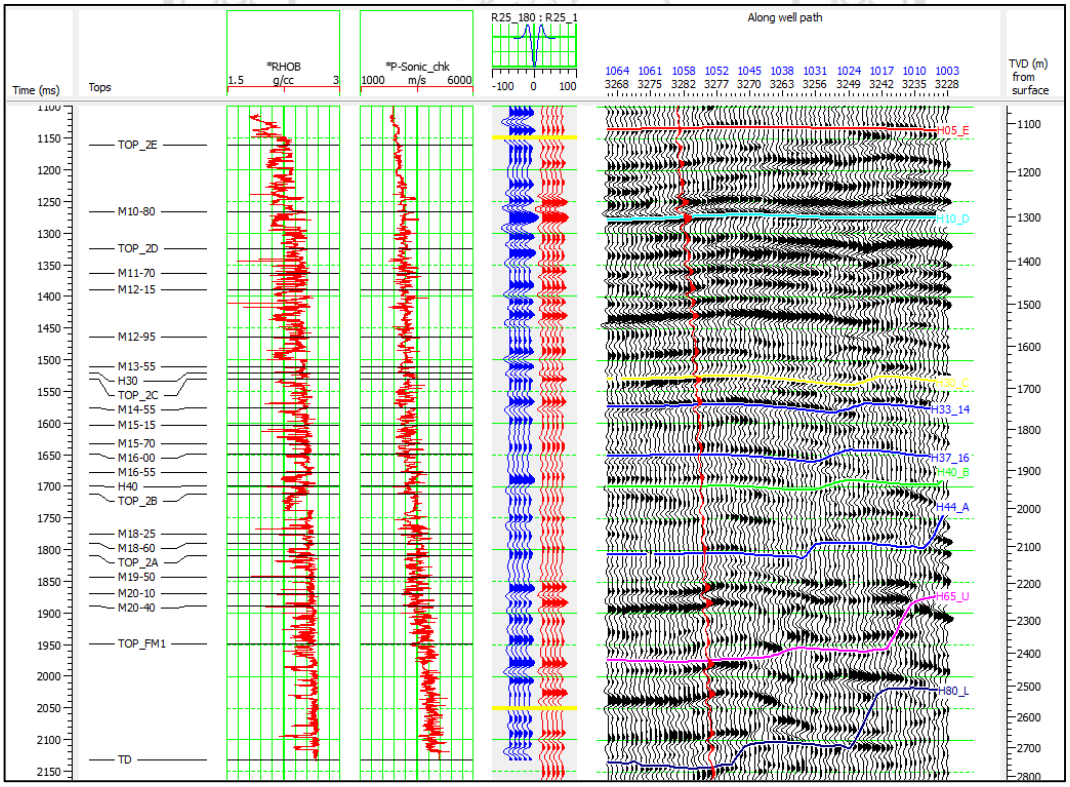

Figure 4-2. Synthetic seismogram and well to seismic correlation of S-2 well showing 75.5% of correlation coefficient after 17 ms of bulk shift

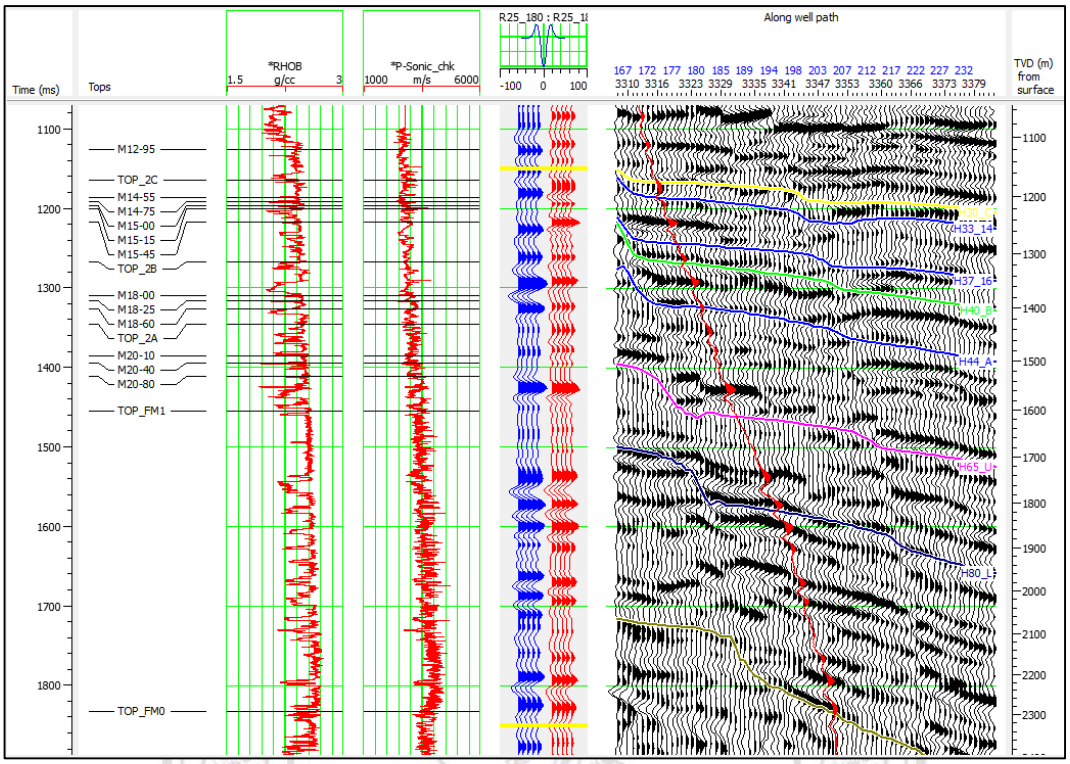

Figure 4-3. Synthetic seismogram and well to seismic correlation of R-2 well showing 53.4% of correlation coefficient after 13 ms of bulk shift

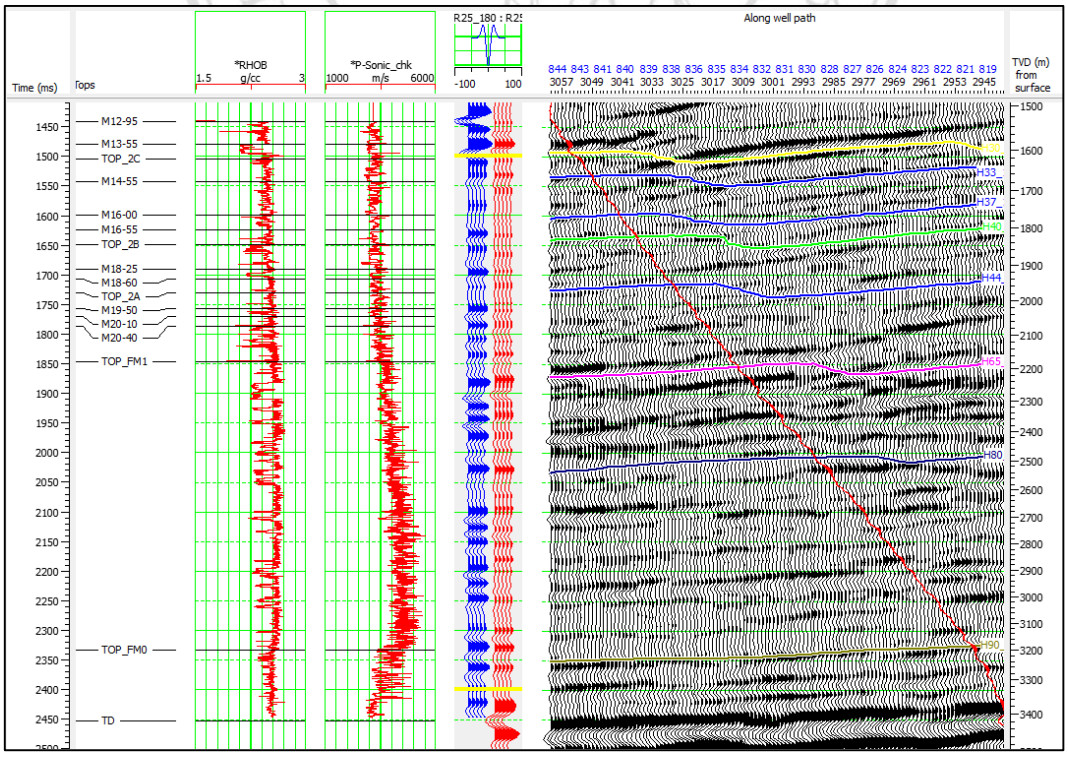

Figure 4-4. Synthetic seismogram and well to seismic correlation of D-36 well showing 65.4% of correlation coefficient after 14 ms of bulk shift

After well to seismic tie is performed, the wavelets which are used for seismic inversion can be extracted from angle gather using wells. The pre-stack inversion should be used few number of wavelets to generate each inverted model because the inversion will be generated based on angle gathers of pre-stack seismic data. The angle gathers of this study are converted from super gathers covering 0 to 45 degrees because incidence angle at the shallow interested reservoirs is up to 45 degree. Therefore, the group of wavelet that was extracted from angle gather using wells in this area (D-36, S-2 and R-2) was divided to 3 wavelets (angle range from 1 to 15, 15 to 30 and 30 to 44). The wavelets were extracted within the interesting zone between horizon E and horizon O plus 500ms (Figure 4-5).

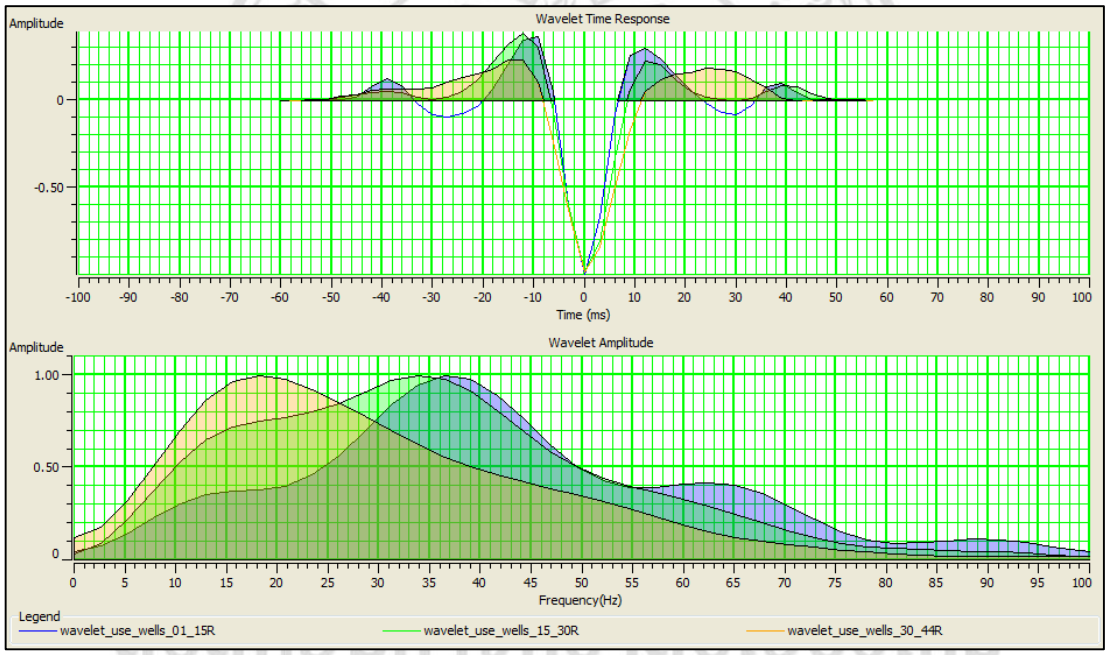

Figure 4-5. A series of wavelets extraction using wells for seismic inversion; Composite trace radius of angle gathers: 1, Angle range: 1 – 44 degree, Wavelet length: 120 ms and Time widow: horizon E to 500 ms below horizon O

4.3 AVO Responds

As description of AVO modeling in Chapter 3 (Figures 3-16 to 3-19), all of sandstone samples are summarized in Table 4-3 which was represented AVO classes with filled fluid and thickness of each fluid layer in Remark column. The "Gas?" (Orange word) is possible gas due to high water saturation and the "Oil?" (Green word) can be whether possible oil or condenses.

Table 4-3. Summary of AVO classes and fluid of each sandstone reservoir

Well	Sandstone	AVO Class	Fluid	Remark
S-2	A	IV	Water	30 m water
	B	II	Water	41 m water
	C	II	Gas, Water	9 m gas and 2 m water (GWC)
	D	II	Gas	9 m gas
R-2	A	IV	Water	20 m water
	B	II	Gas	20 m gas
	C	II	Gas, Oil?, Water	9 m gas, 6 m oil? and 2 m water (GFC)
	D	II	Gas? Gas, Water	1st layer: 6 m gas? 2nd layer: 11 m gas and 5 m water (GWC) Stacked sandstone
D-36	A	IV	Water	19 m water
	B	IV	Water	44 m water
	C	IV	Gas, Water	5 m gas and 11 m water (GWC)
	D	II	Gas?	12 m gas?
	E	IIp	Gas	5 m gas

Remark: GWC is gas water contact, and GFC is gas fluid contact

4.4 Initial Strata Model

The strata initial models for seismic inversion were generated from geometries of angle gathers, existing wells and picking seismic horizons as guides to extrapolate well logs between wells. These models try to define the geological properties using seismic parameter such as velocity, reflectivity or impedance similar to stratigraphic model.

The P-impedance and S-impedance initial models were generated from well data (P-sonic, S-sonic and density logs) combining stacking velocity. The initial model using the both velocity sources was compared to the model using only velocity from wells and was shown better image and correction of stratigraphy. At position close to well, the values of P-impedance models are similar in both models. In contrast, at the location far from well and unavailable well log data, the values are much different because the values of P-impedance models using only well velocity are interpolated from nearby available data. Moreover, the frequency content of stacking velocity is from 0 to 2 Hz, and initial model from well log cover frequencies higher than 2 till 10 Hz. It is too important to add both initial model created by stacking velocity and initial model from well log to be final models for applying to seismic inversion.

To decide frequency bandwidth for creating the initial model, amplitude spectrum had been extracted from seismic data. The amplitude spectrum represents low frequency up to12 Hz (Figure 4-6). Therefore, low-pass frequency filter should be applied to filter all frequency above 12 Hz, high-cut frequency should be 9 Hz and taper should be 12 Hz that mean the characteristic filter is (0, 0, 9, 12). The filter result displays no visible signal, so it should be used to create the initial model (Figure 4-7). If more signal show, they will normally include high frequency and will disturb low frequency model.

The models that were built are P-impedance, S-impedance, P-wave velocity, S-wave velocity density and V_P/V_S models (Figures 4-8 to 4-10). These models and original well logs will be applied to inversion analysis for generating preliminary inverted logs, and then they were input to pre-stack inversion models.

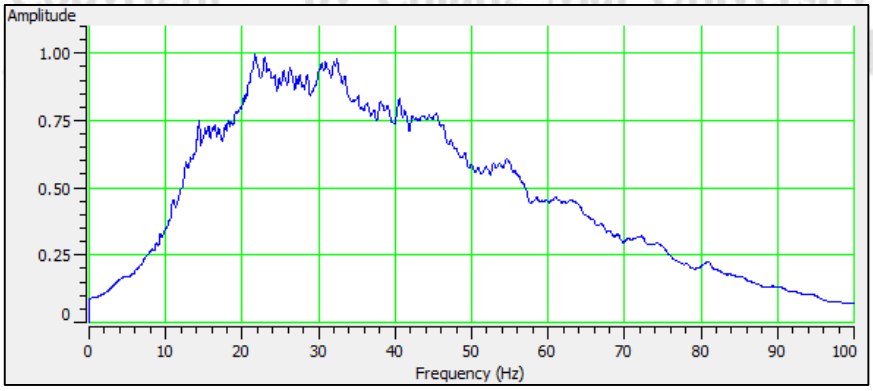

Figure 4-6. Amplitude spectrum extracting from seismic data represent the low frequency up to 12 Hz.

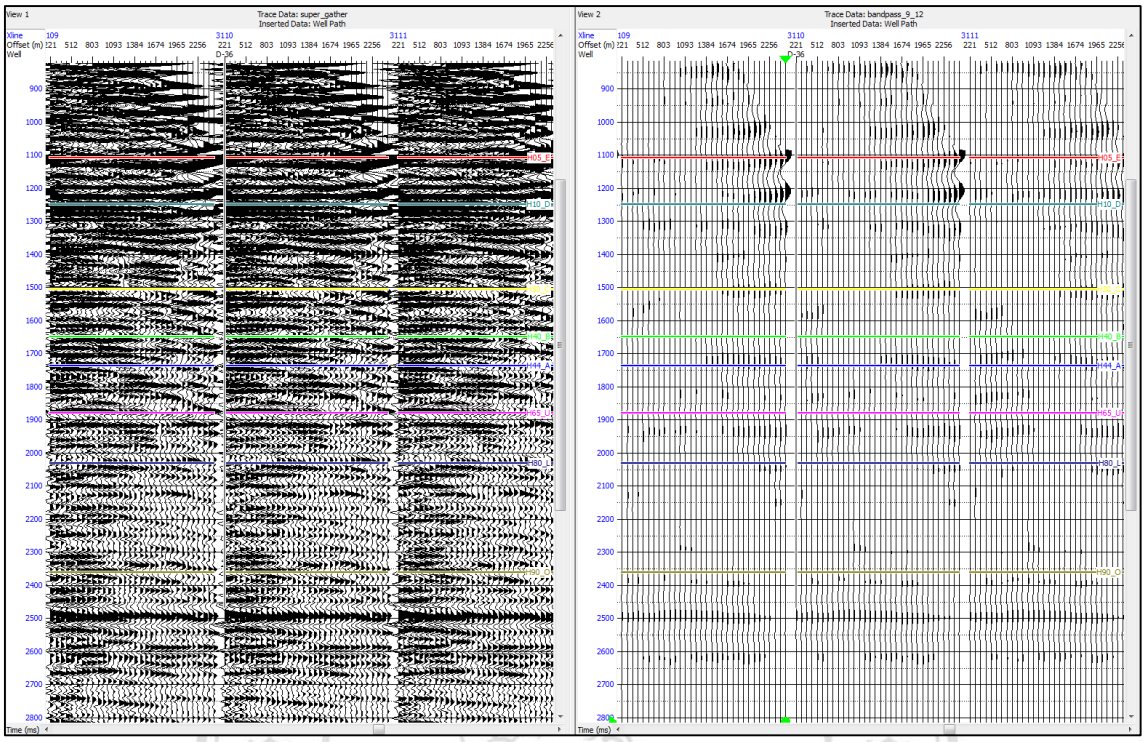

Figure 4-7. Seismic super gathers comparing to low pass frequency filter gathers, high cut frequency is 9 Hz and taper is 12 Hz that characteristic filter is (0, 0, 9, 12).

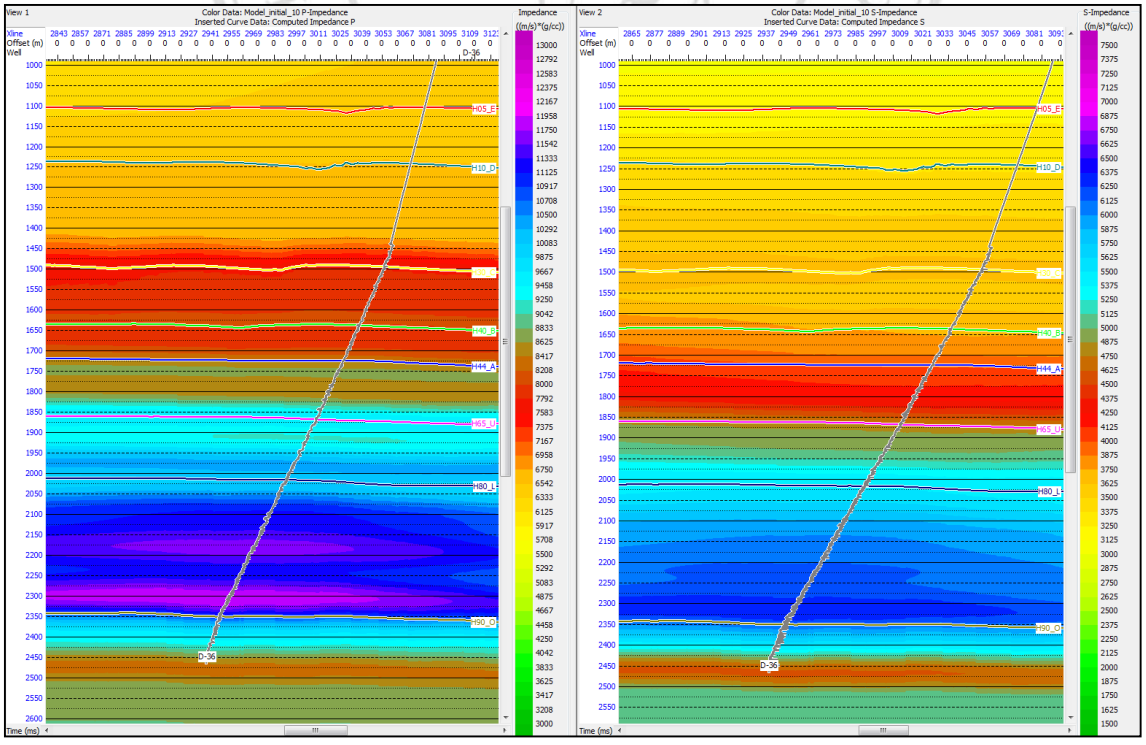

Figure 4-8. P-impedance initial strata model (left) and S-impedance initial strata model (right) using stacking velocity and well data

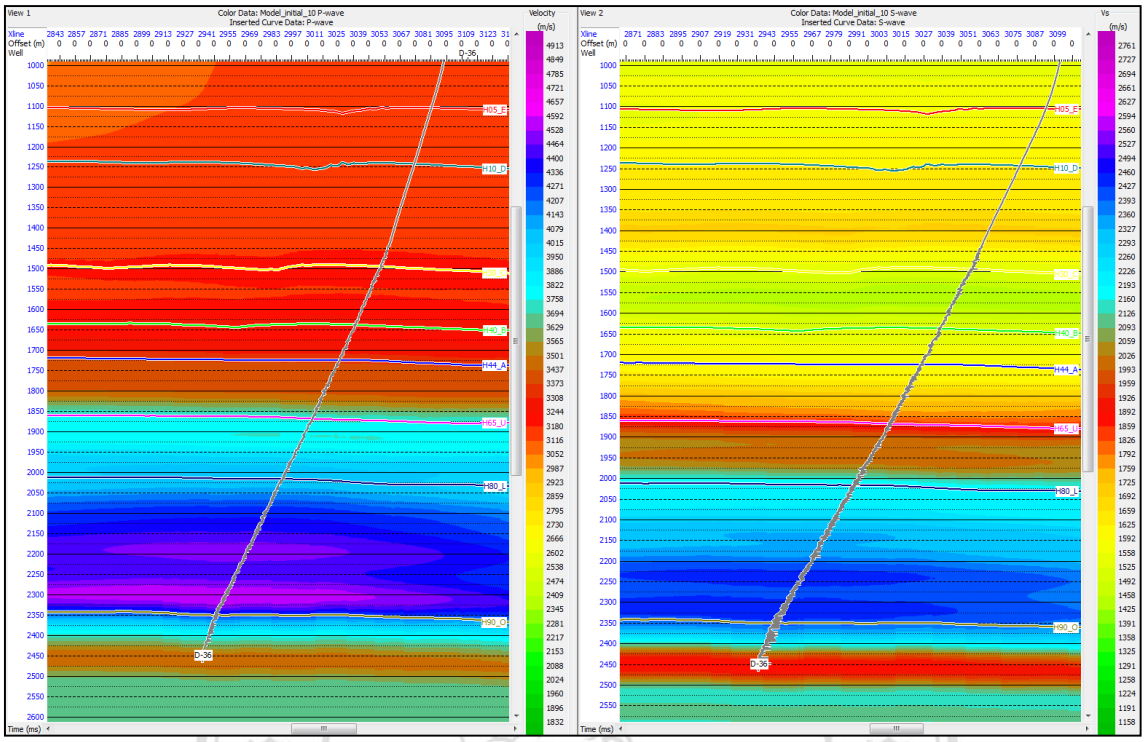

Figure 4-9. P-wave initial strata model (left) and S-wave initial strata model (right) using stacking velocity and well data

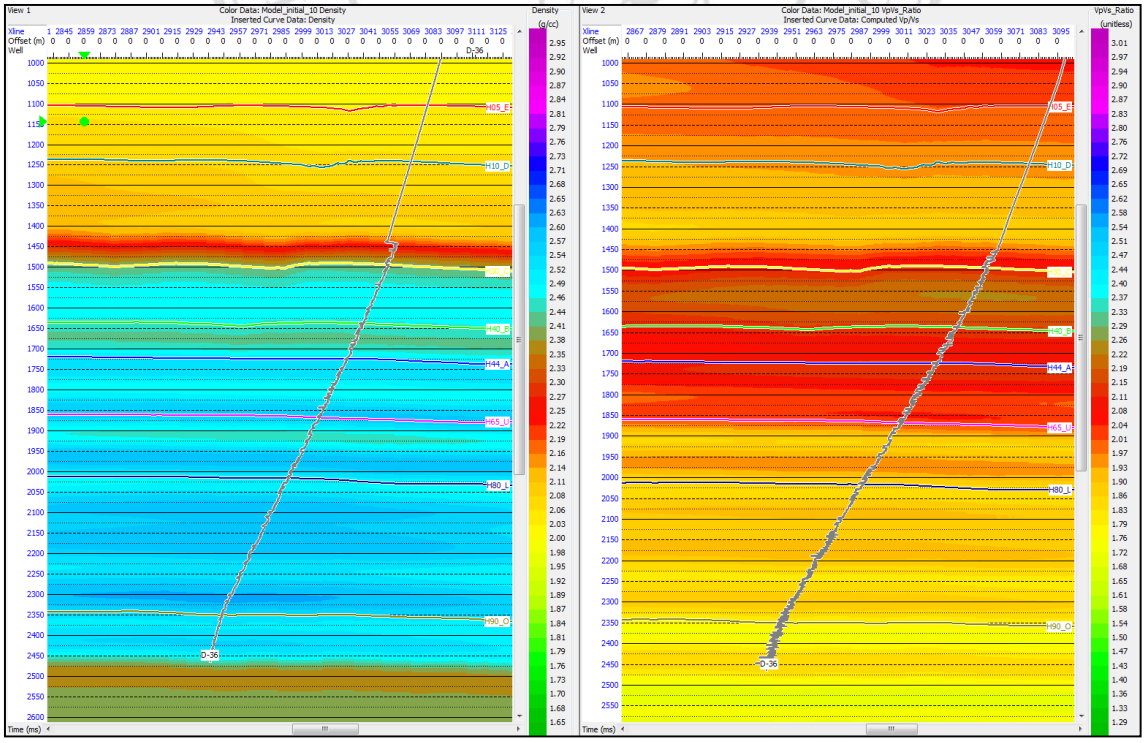

Figure 4-10. Density initial strata model (left) and V_P/V_S initial strata model (right) using stacking velocity and well data

4.5 Inversion Analysis

The inversion analysis was performed for testing the parameters of seismic inversion at well locations, and then they were determined for applying to seismic volume. The best parameters that were already tested and selected are represented in Table 4-4. The regression coefficients and preliminary pre-whitening values were derived from crossplot between natural logarithm of P-impedance [$\ln(Z_P)$] and both natural logarithm S-impedance [$\ln(Z_S)$] and natural logarithm density [ln(Dn)] (Figure 4-11). The pre-whitening values can be modified to optimize the correlation and error values of inversion analysis.

Table 4-4. Summary of inversion parameters using for pre-stack seismic inversion

Regression Coefficients	**ln(Zs) = k * ln(Zp) + kc**	
	k	1.14923
	kc	-1.99334
	ln(Dn) = m * ln(Zp) + mc	
	m	0.363162
	mc	-2.42028
Background Ratio (Vs/Vp)	Gamma	0.5
Pre-whitening	Method	Covariance
	ln(Zp)	0.140193
	delta ln(Zs)	0.115189
	delta ln(density)	0.0574668
	Pre-whitening value	1%
Muted or Dead Traces Handling	Assume a trace is completely dead if it has less than 10% lives samples	
Number of Iterations	50	
Scalar	Calculate and apply separate scalars for each CDP	
	Adjustment factor	1
Composite Trace	Capture option	Neighborhood
	Neighborhood Radius	5

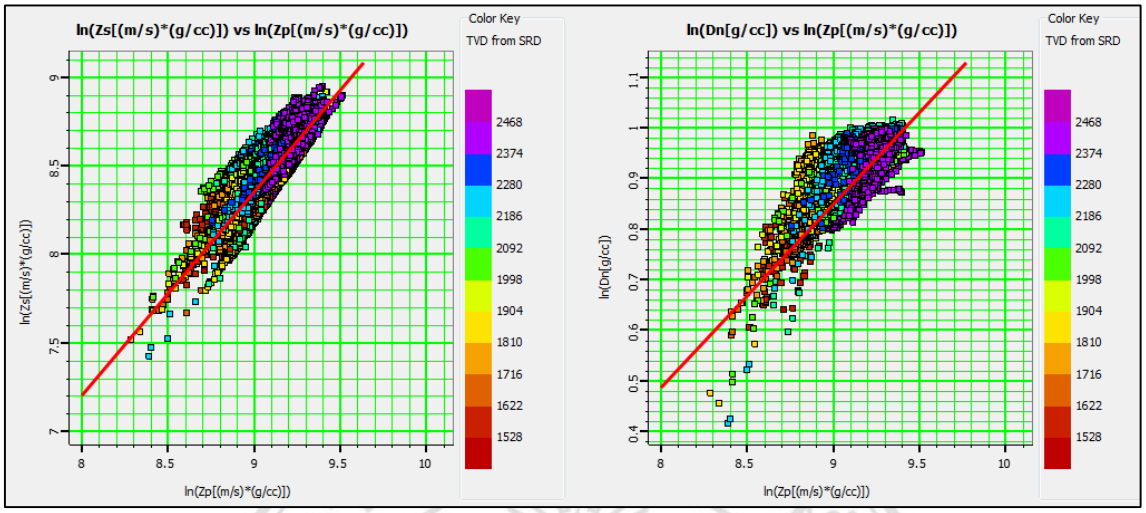

Figure 4-11. Crossplot between ln(Z_P) and ln(Z_S) (left) and between ln(Z_P) and ln(Dn) (right), the both red lines can be moved for deriving the regression coefficients and the pre-whitening values.

The inversion analysis of each well was comparison of original well logs (blue curves), inverted well log and (red curves) and initial model at wells (black curves) which the well logs are Z_P, Z_S, density and V_P/V_S ratio. Moreover, the inverted synthetic traces and error traces comparing to seismic traces were also represented in the inversion analysis (Figures 4-12 to 4-14). The inverted synthetic traces were generated form the well logs convolving with the extracted wavelet of D-36 well. They were represented to correlation and error values, and were summarized in Table 4-5 together with the error values of well logs.

Table 4-5. Error values between original well log and inverted well log together with correlation and error values of inverted synthetic comparing to seismic traces

Well	Error of Z_P	Error of Z_S	Error of density	Error of V_P/V_S	Inverted Synthetic Correlation
D-36	737.0	411.8	0.0877	0.0966	0.889931
R-2	749.1	451.0	0.1007	0.1374	0.919716
S-2	744.5	575.0	0.0937	0.1190	0.906409

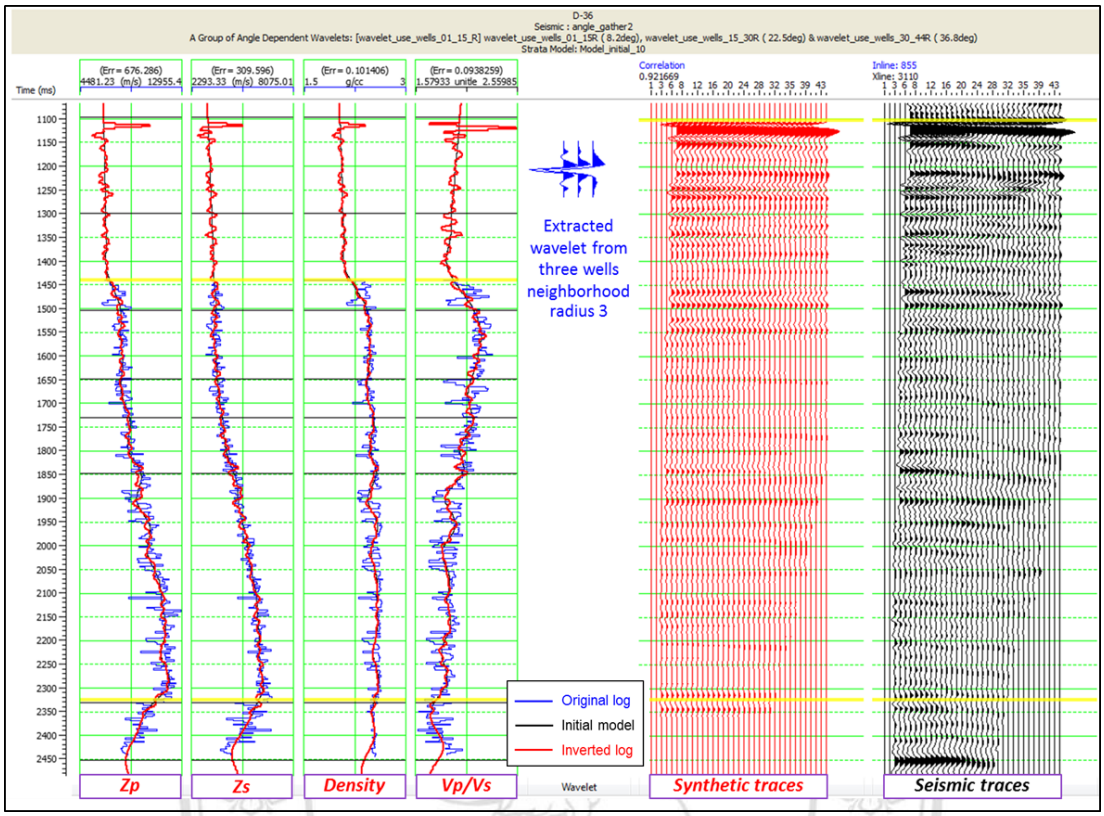

Figure 4-12. Inversion analysis at D-36 well

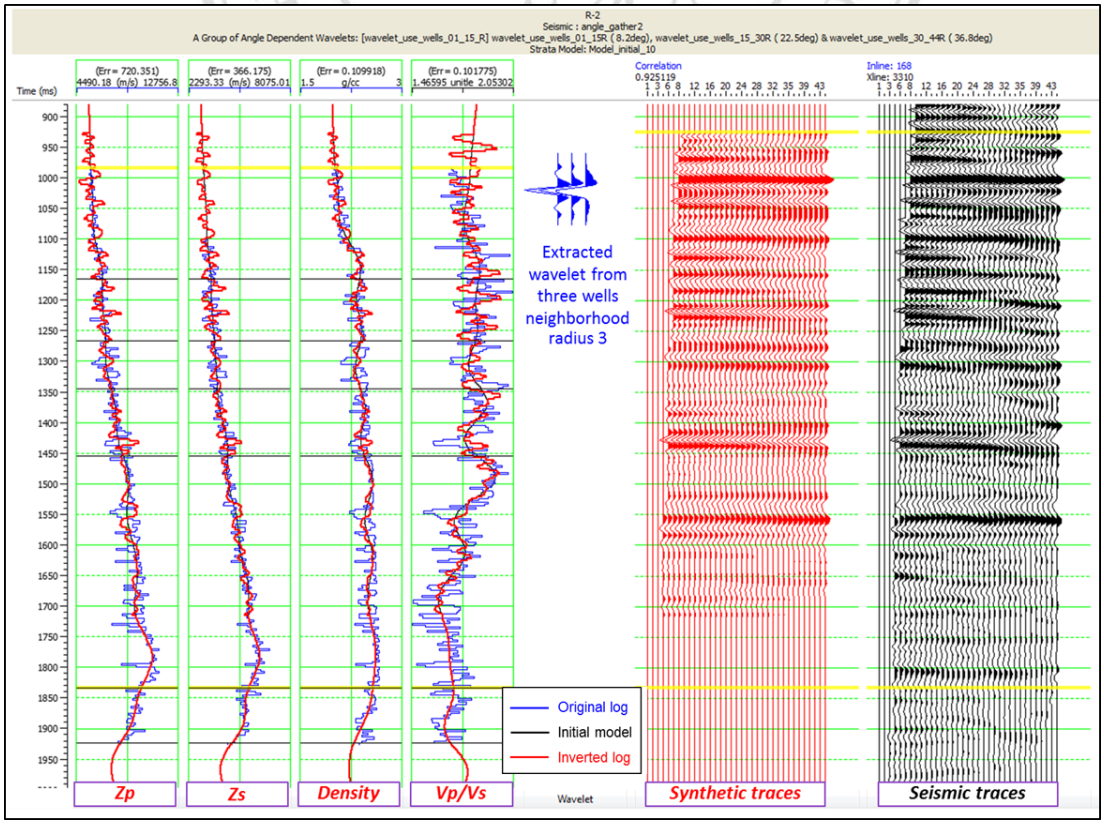

Figure 4-13. Inversion analysis at R-2 well

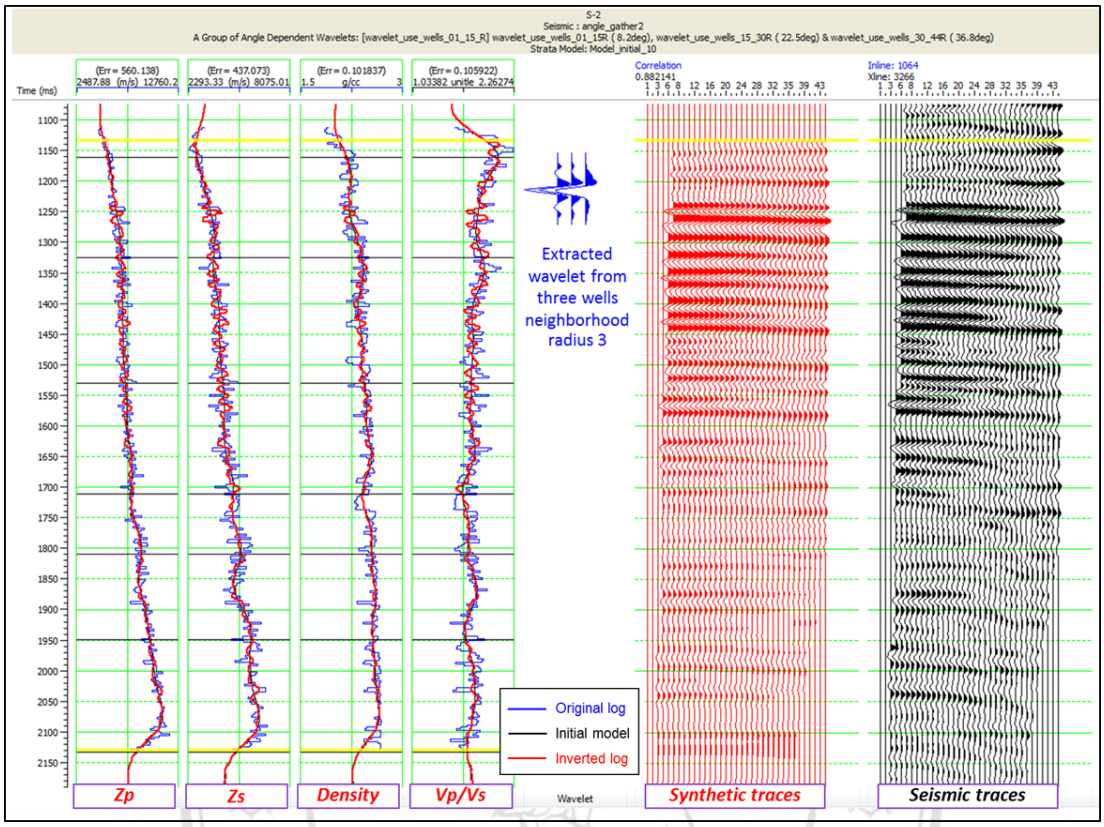

Figure 4-14. Inversion analysis at S-2 well

4.6 Pre-stack Seismic Inversion

In this study, the pre-stack seismic simultaneous inversion was run in Hampson-Russell Suite Software. It is a combination of three outputs which are acoustic impedance (Z_P), shear impedance (Z_S) and density, so inverted V_P/V_S is also calculated from them. Inversion results of each inverted model showing on sections along wells were used to QC measurement before applying to seismic volume. The inversion log curves and color bands at wells were overlaid the inverted sections with same types of inversion and color scale (Figures 4-15 to 4-17). Each inverted section of D-36 and R-2 well quite matches with well logs more than S-2 because the S-2 well was located near boundary of seismic data, so it may be effected during migration and fewer binning fold. The inversion was computed to volumes of Z_P, Zs, density and V_P/V_S after optimum parameters was tested and selected. The inversion results are generally very encouraging, and the match between the inverted seismic result and the well logs is generally good with respect to both reflector placement and inverted values.

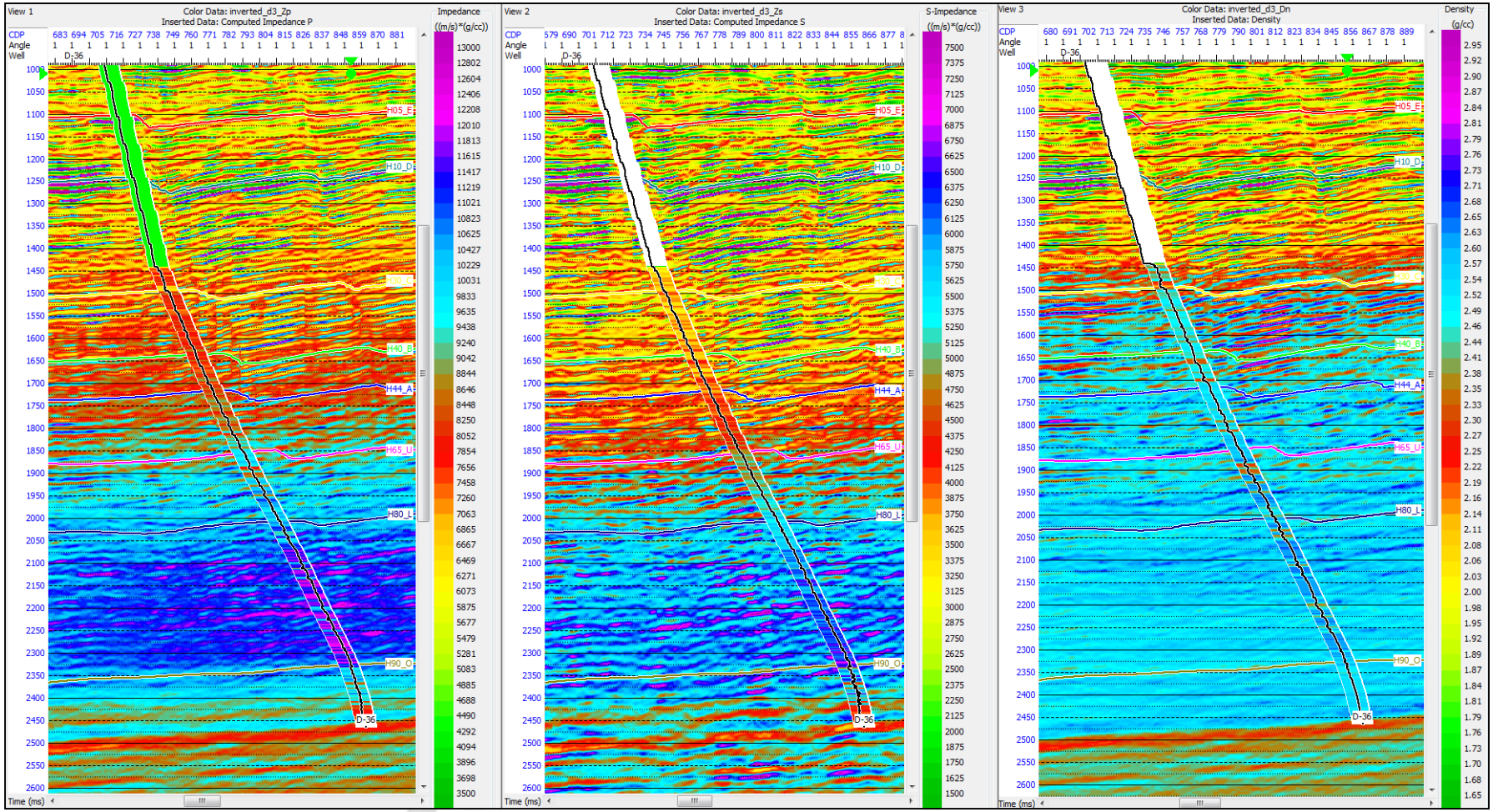

Figure 4-15. Sections of inverted Z_P (left), inverted Z_S (middle) and inverted density (right) along D-36 well overlying with their well logs

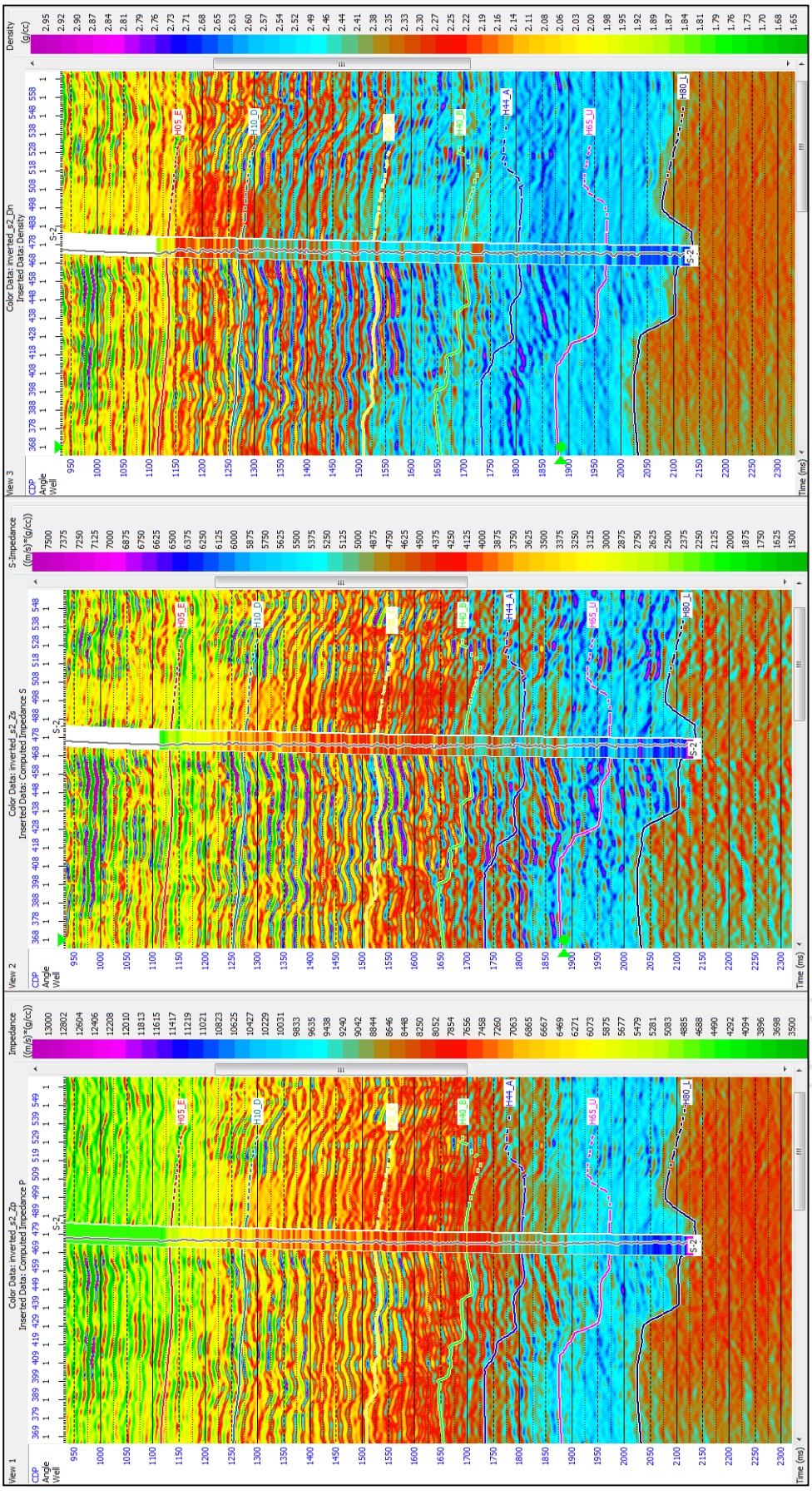

Figure 4-16. Sections of inverted Z_P (left), inverted Z_S (middle) and inverted density (right) along S-2 well overlying with their well logs

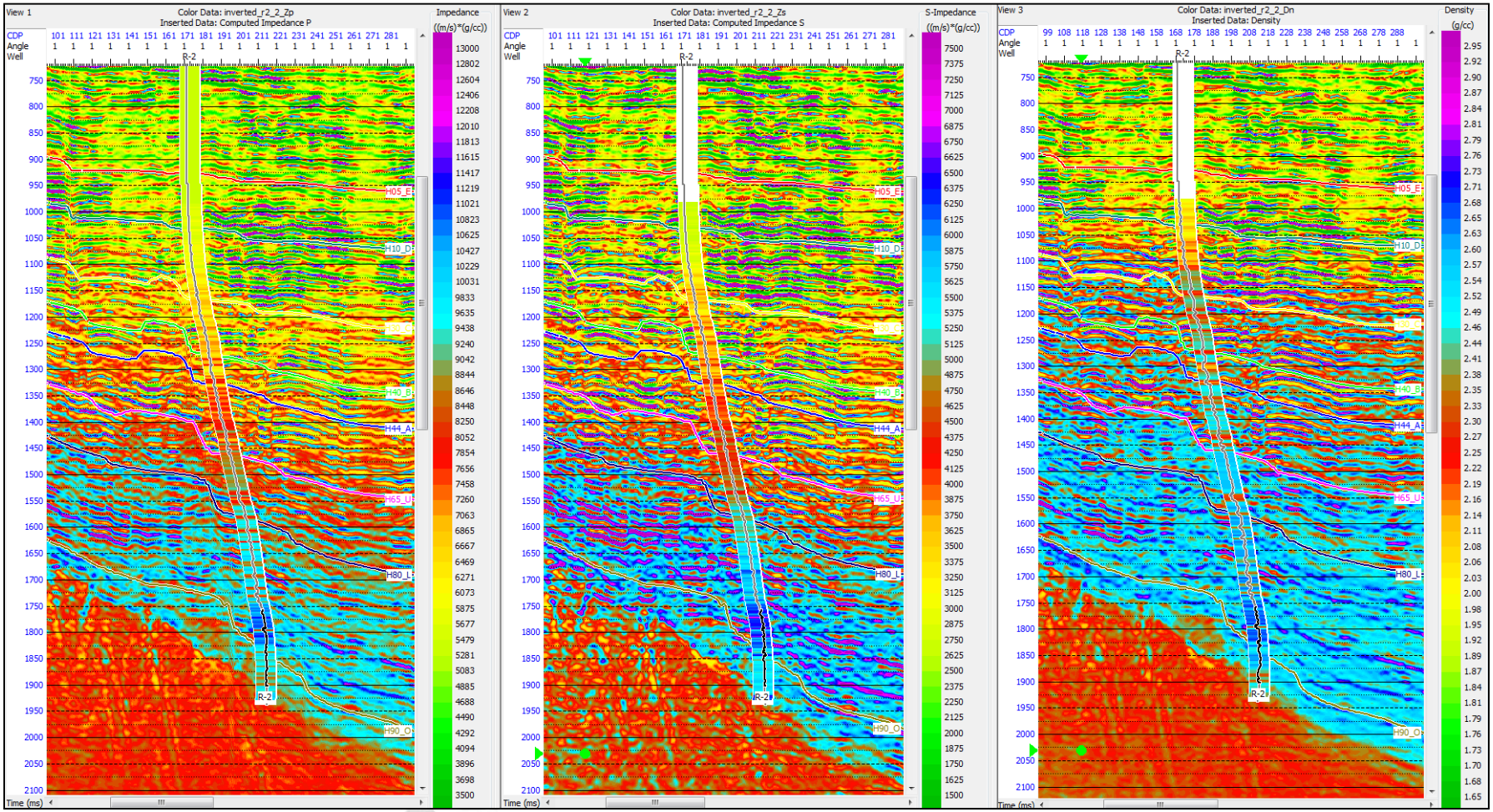

Figure 4-17. Sections of inverted Z_P (left), inverted Z_S (middle) and inverted density (right) along R-2 well overlying with their well logs

4.7 Lithology Delineation

Lithology delineation was predicted and described using seismic inversion models which are comprised of P-impedance (Z_P), S-impedance (Z_S), density and V_P/V_S. Horizon slices for different physical properties were obtained that are used to observe lateral distribution of lithology along horizons (Figure 4-18 and Figure 4-19). However, based on these horizon slices prediction of the lithology is not easy, so the color scale of them should be modified for each interesting interval. After each color scale of horizon slice was changed, the lithology can be typically delineated to sandstone with low impedances and low density. For example in Figure 4-19, the horizon slices of horizon O were extracted from seismic inversion volumes and were changed the color scales. In the slices of Z_P, Z_S and density, low values (yellow, red and brown color) should be predicted to sandstone and are represented to channel trends in yellow dash lines. In contrast, V_P/V_S slice of this horizon does not show any patterns. D-36 well (in white circle) was penetrated to this horizon and found thin gas sand (2.9 m) near predicted channel trend, but it is rarely evidence to ascertain the lithology.

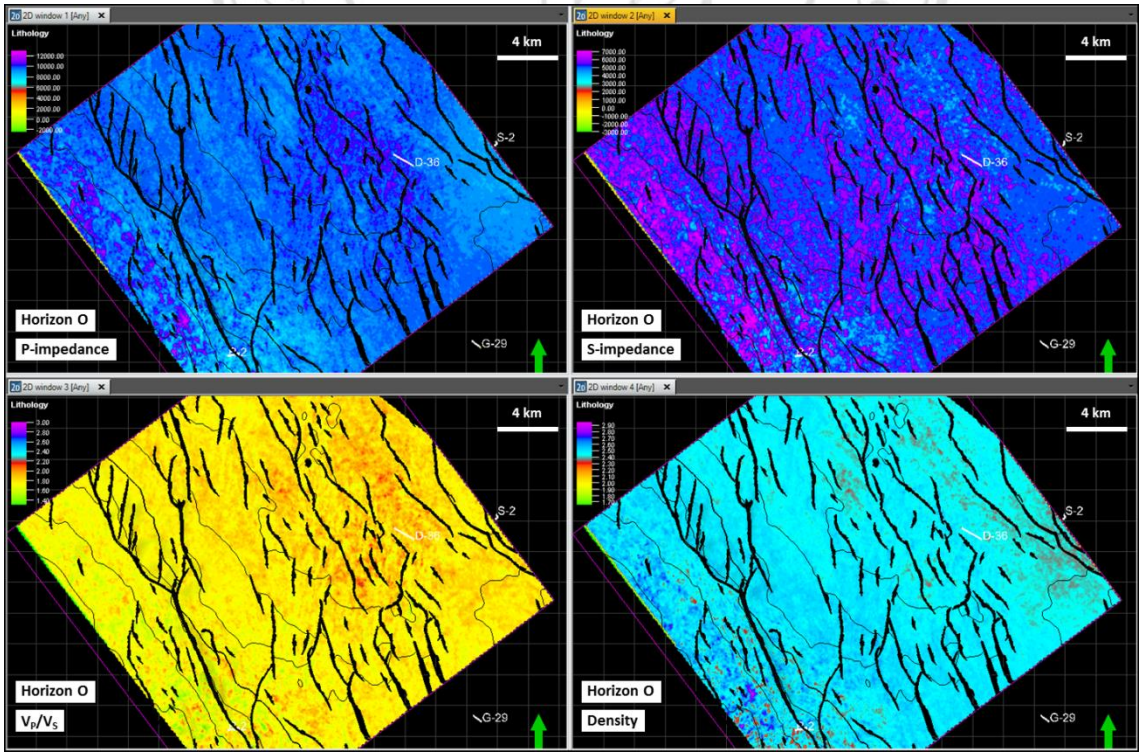

Figure 4-18. The horizon slices of horizon O (top Oligocene) extracting from inversion models of Z_P, Z_S, density and V_P/V_S

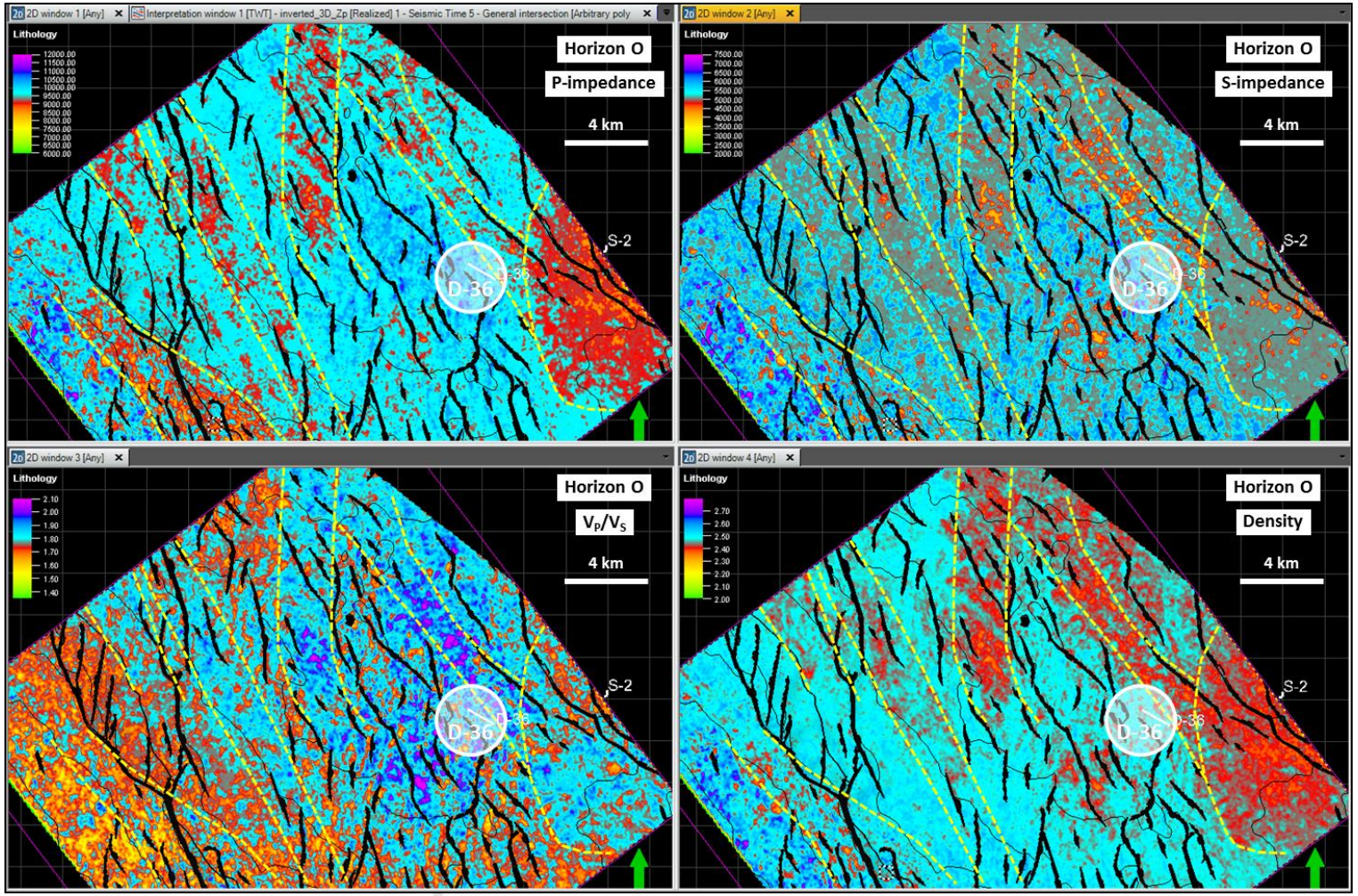

Figure 4-19. The horizon slices of horizon O (top Oligocene or FM0) extracting from inversion models of Z_P, Z_S, density and V_P/V_S after changing color scale overlying by predicted channel sand trends (yellow dash line) of low Z_P, Z_S and density

Similarly, the inversion slices of horizon O+34 that were extracted from inversion volume at 34 ms below horizon O were displayed unpattern in V_P/V_S map and low value in east of Z_P, Z_S and density map (Figure 4-20). D-36 well also found 5 m thickness of gas sand (sand E of D-36 in Chapter 3) at this interval near low impedances and low density area.

In formation 1 (FM1), the horizon slices of horizon U which located at top of FM1 were also extracted from seismic inversion volumes. Map of Z_P, Z_S and density are represented low value trends which were predicted to sand channels in northwest-southeast trends (Figure 4-21). D-36 well where penetrates near edge of the predicted east channel (in white circle) was reported to 1 m thickness of water sandstone. This is possible to be corresponded to high value in V_P/V_S map.

In formation 2, surface attribute through horizon C was extracted to get horizon slices of Z_P, Z_S, density and V_P/V_S. Low impedances and low density value trends are estimated to be sand channel in north-south direction (within yellow dash line of Figure 4-22). In these trends, V_P/V_S map represents relative high values. Water sandstone with 19 m thickness was found in of D-36 well (in white circle) near east channel (400 m far), but it is less reliable evidence to convince these low value trends to sandstone.

Another horizon slice in formation 2 is horizon U-23 which was extracted from each inversion volume at 23 ms above horizon U. This horizon is near top FM1. The low values of Z_P, Z_S and density maps in this horizon slice were also interpreted to channel trends and predicted to sand channel (Figure 4-23). R-2 well found 19 m thickness of gas sand (in white circle) but V_P/V_S map does not shown low values relating to gas.

For all examples of horizon slices, they are hard to estimate sand channel trends and difficult to predict lithology based on these seismic inversion models and few well information. The problems that can be affected to seismic inversion are vertical limited resolution of seismic to thin layers of lithology, initial seismic acquisition parameters and also seismic inversion parameters during performing each process.

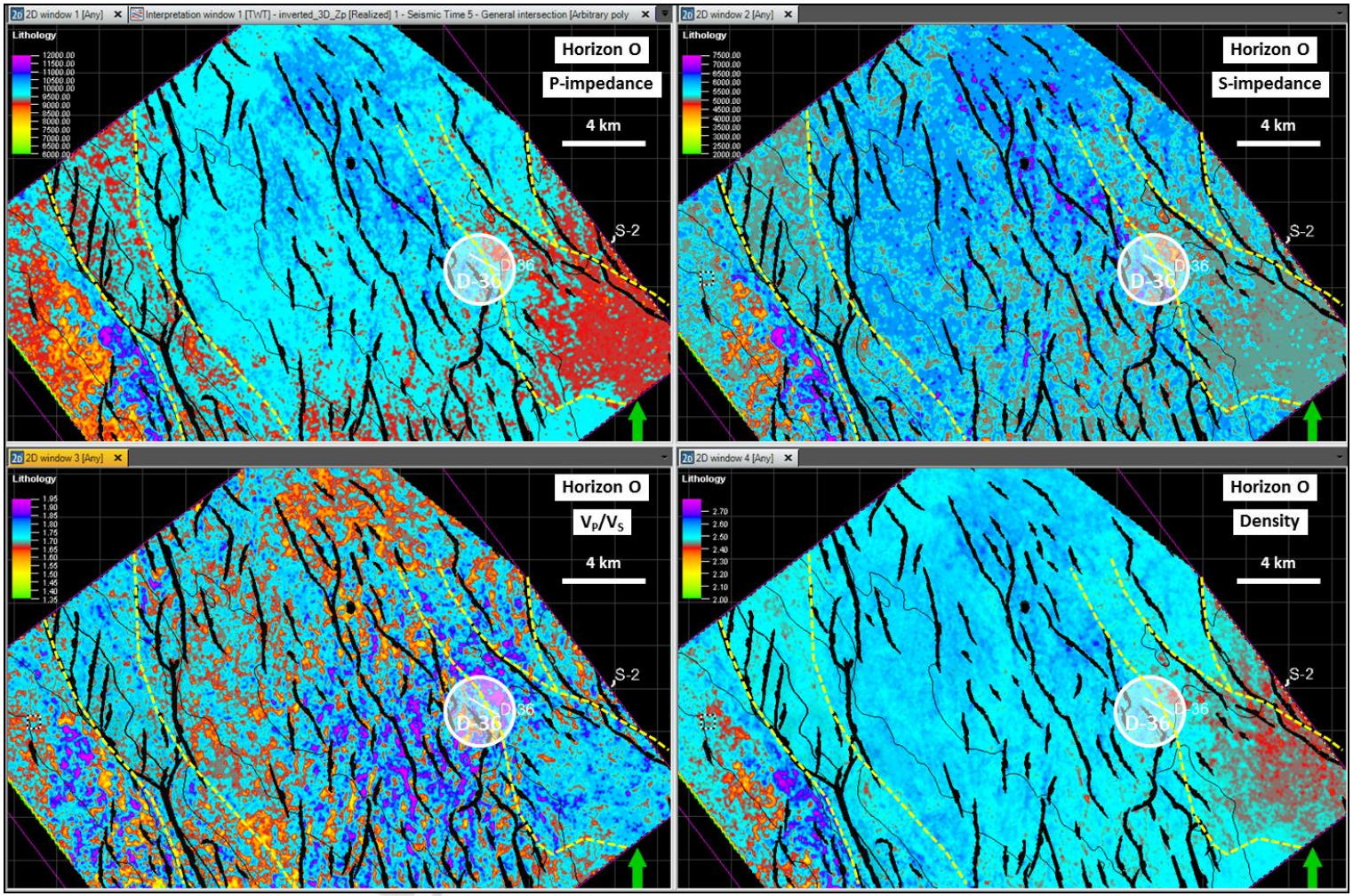

Figure 4-20. The horizon slices of horizon O+34 ms extracting from inversion models of Z_P, Z_S, density and V_P/V_S and changing color scale overlying by predicted channel sand trends (yellow dash line) of low Z_P, Z_S and density

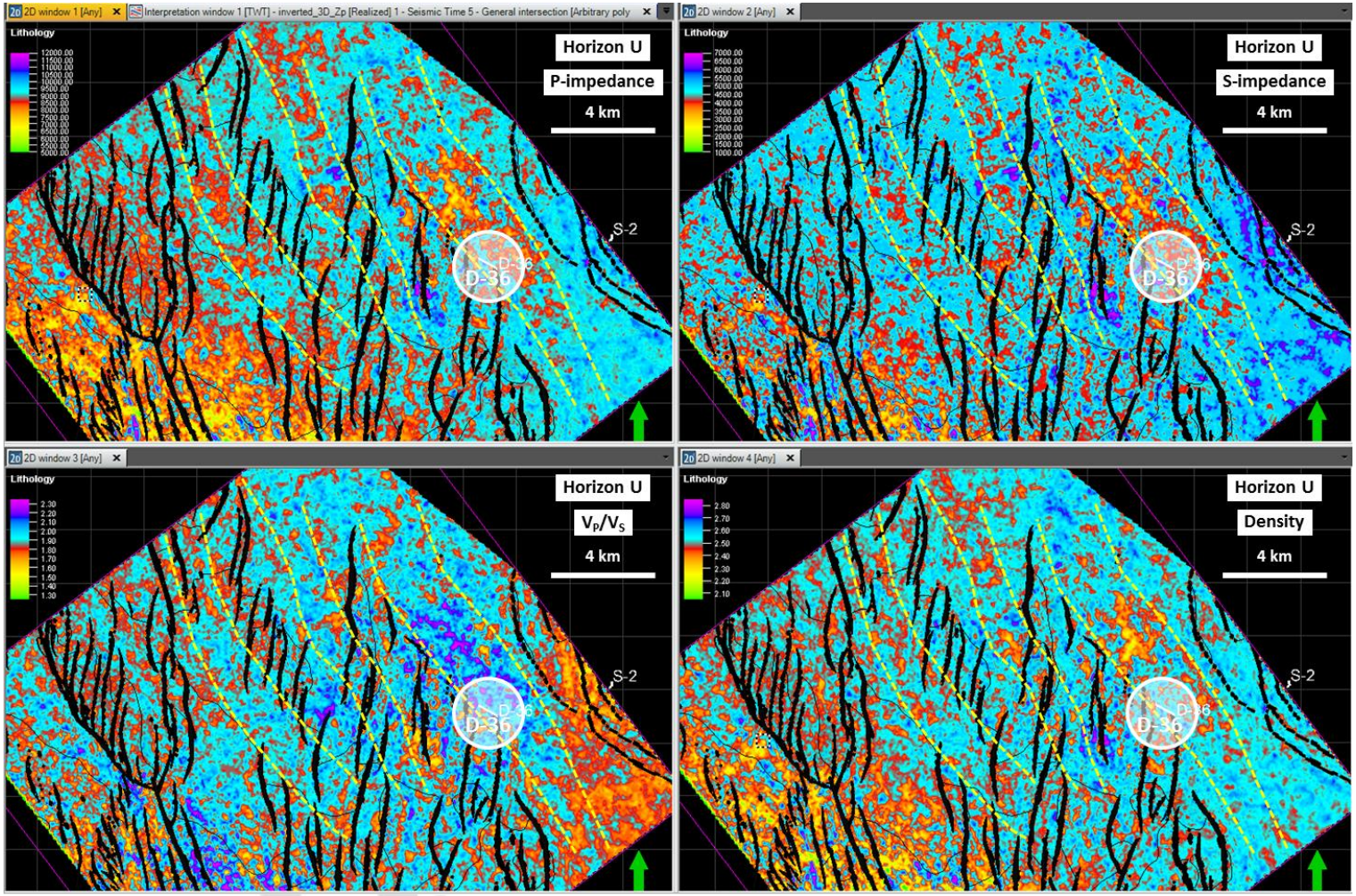

Figure 4-21. The horizon slices of horizon U (top FM1) extracting from inversion models of Z_P, Z_S, density and V_P/V_S after changing color scale overlying by predicted channel sand trends (yellow dash line) of low Z_P, Z_S and density

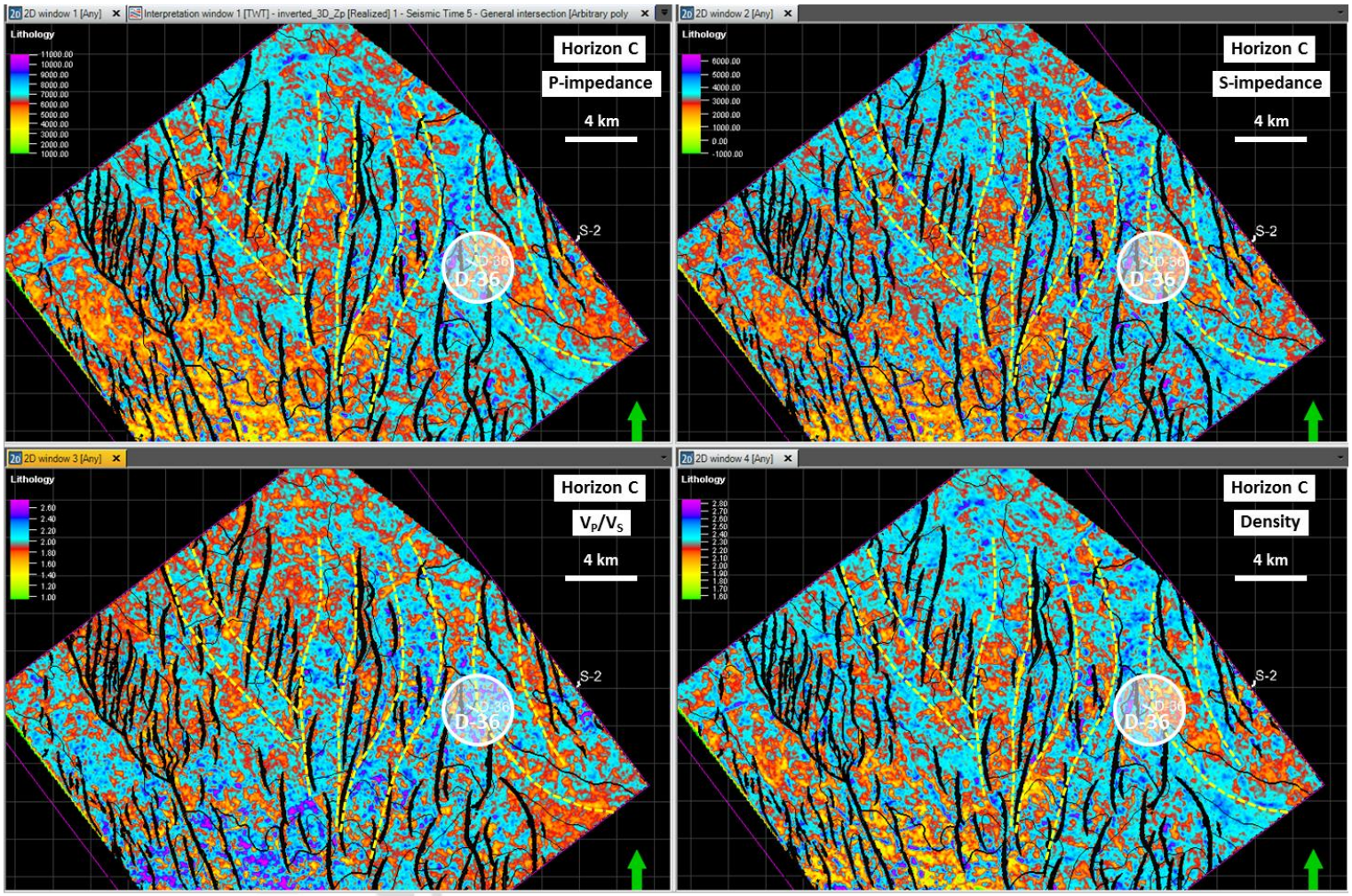

Figure 4-22. The horizon slices of horizon C (top Unit 2C) extracting from inversion models of Z_P, Z_S, density and V_P/V_S after changing color scale overlying by predicted channel sand trends (yellow dash line) of low Z_P, Z_S and density

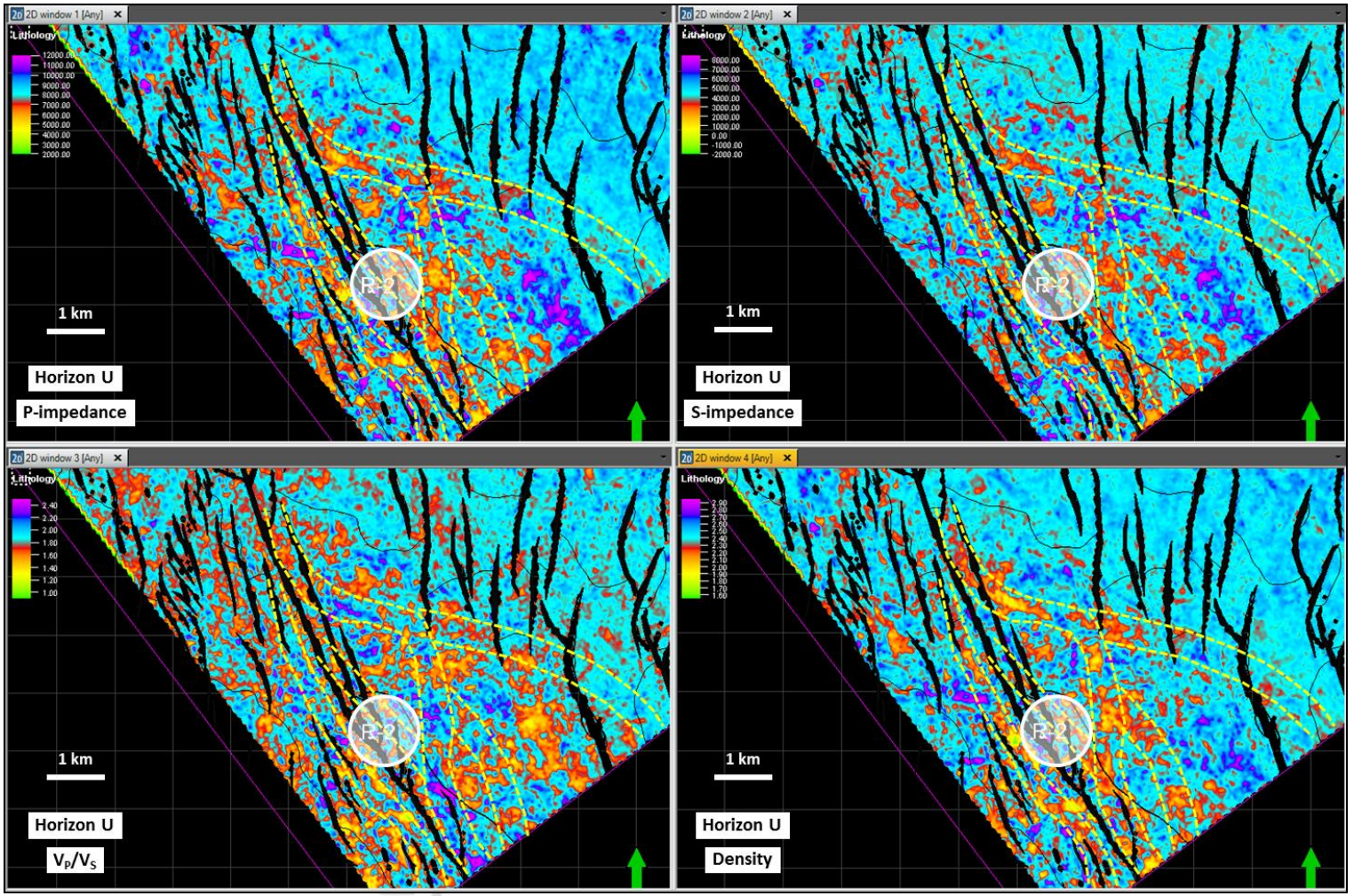

Figure 4-23. The horizon slices of horizon U-23 ms extracting from inversion models of Z_P, Z_S, density and V_P/V_S and changing color scale overlying by predicted channel sand trends (yellow dash line) of low Z_P, Z_S and density